

1
2
3
4
5
6
7
8
9
10
11
12
13
14
15

**Changing Seasonality of Annual Maximum Floods over the Conterminous
US: Potential Drivers and Regional Synthesis**

Bidroha Basu¹, Rajarshi Das Bhowmik², and A. Sankarasubramanian^{3,*}

¹School of Architecture, Planning & Environmental Policy, University College Dublin, Dublin,
Ireland.

²Department of Civil Engineering, Indian Institute of Science, Bangalore, India.

³Department of Civil, Construction and Environmental Engineering, North Carolina State
University, Raleigh NC 27695-7908

* - Corresponding author's email address: sankar_arumugam@ncsu.edu

16 **Abstract**

17 Understanding the flood generating mechanisms that influence flood seasonality in a region
18 provides information on setting up relevant contingency measures. While former studies had
19 estimated flood seasonality at regional/continental scale, limited/no studies had investigated the
20 climate/basin drivers that influence the changes in flood seasonality. Considering this, the current
21 study performed two analysis i) estimated the changes in the seasonality of annual maximum
22 floods (AMF) between pre- and post-1970 across Hydroclimate Data Network basins over the
23 coterminous United States, and ii) identified the predictors that influence the change in the
24 seasonality from a set of climate and geomorphic variables. Significant changes in the AMF
25 seasonality were noted for approximately half of the basins in the eastern US while low to no
26 change was found in a majority of the basins in the central/western US. We found that a decrease
27 (increase) in the seasonality index, indicating floods arriving more uniformly (more concentrated
28 in time), is typically associated with an increase in the precipitation (temperature) in basins
29 where a strong change in flood seasonality occurs. Elevation has a more dominant role as
30 compared to the drainage area in changing the flood seasonality as the former affects the form of
31 precipitation in basins in higher elevations. This is particularly true for western US where floods
32 arrive more distributed over the year (i.e., decrease in flood seasonality index), which potentially
33 indicates increased warming resulting in early snowmelt.

34

35 **1. Introduction**

36 Among the natural disasters, floods are the most damaging disasters resulting in
37 significant loss of human life and property (Ohl et al., 2000; WHO, 2002; Jonkman, 2005).
38 Several studies have predicted that the frequency of floods is likely to increase in the near future
39 under global climate change (Yin et al., 2018), while a few studies found no strong evidence of
40 an association between increased temperature and increased flooding (Wasko et al., 2019).
41 Nevertheless, regions that are severely affected by recurring floods require information on the
42 flood potential in the following seasons, thereby providing a basis for setting up contingency
43 measures (Sankarasubramanian and Lall, 2003). Hence, it is of great importance to understand
44 flood generating mechanisms of annual maximum floods (AMF) for ensuring reliable flood
45 prediction and effective mitigation. In this context, one particular statistical attribute of
46 importance is the seasonality of AMFs in a given basin/region (e.g., Villarini, 2015; Li et al.,
47 2016). Analysis of flood seasonality and their temporal changes will provide us critical
48 information on the changing flood risk at the national scale (McCabe and Clark, 2005; Nakamura
49 et al., 2013).

50 Recently, Villarini (2015) and Ye et al., (2017) summarized the flood seasonality and
51 their changes over the coterminous US (CONUS). Villarini (2015) showed a strong seasonality
52 in flooding exists across the CONUS, with floods occurring during October to March across the
53 western and eastern US and is concentrated in the post-winter (April to May) season in the snow-
54 dominated basins. Villarini (2015) analyzed flood seasonality over 7506 USGS stations,
55 consisting of natural and controlled basins, and found that the changes in flood seasonality is
56 significant, as expected, in controlled basins. In a similar study for Great Britain, Black and
57 Werritty (1997) found that the majority of floods (around 78%) in the country occur during the

58 October to March period. In southern Canada, Cunderlik and Ouardaa (2009) reported early
59 occurrence of spring floods due to snowmelt from warming temperature (Peterson et al., 2012).
60 However, the study did not find a strong signal related to the timing of the fall floods. Ye et al.,
61 (2017) analyzed the changes in AMF seasonality over 250 natural basins from the MOPEX
62 dataset over the CONUS and found that changes in annual maximum rainfall and antecedent
63 storage conditions impact the shift in seasonality. Apart from annual maximum floods, studies
64 have also investigated the streamflow seasonality over the US (Regonda et al., 2004; Petersen et
65 al., 2012). Regonda et al. (2004) found evidence of early spring temperature spells and early
66 occurrence of peak snowmelt which shifts the spring flow timing. Based on the review of
67 existing literature, we understand that i) significant spatial variability in flood seasonality exists
68 in natural basins across the CONUS, ii) the consensus on the large-scale drivers of changes in
69 flood seasonality is still not clear as studies considered only limited basins (e.g., Ye et al., 2017) .
70 The current study augments the findings of Villarni (2015) and Ye et al., (2017) by considering
71 more natural basins (975 stations) from the USGS Hydroclimate Data Network (HCDN) and by
72 associating the drivers of changes in flood seasonality with hydroclimatic variables and basin
73 characteristics. We also synthesize the changes in seasonality and the associated drivers on a
74 regional basis over the CONUS.

75 Previous studies investigated the dominant drivers of the seasonality of floods from both
76 moisture transport and teleconnection perspective as well as in understanding the role of
77 hydroclimatology of the basin. Flood magnitudes and their dominant season of occurrence have
78 been attributed to oceanic conditions (e.g., El-Nino Southern Oscillation and Pacific Decadal
79 Oscillation conditions), basin-level climatic conditions (e.g., precipitation) and land surface
80 states (e.g., snowpack) (Pizarro and Lall, 2002; Steinschneider and Lall, 2016; Ye et al., 2017).

81 Basin characteristics (such as drainage area and elevation) also contribute to the shift in
82 seasonality due to changes in the hydroclimatic patterns. Several studies have shown that it is the
83 scale (i.e., the drainage area) which predominantly explain the spatial variability in the
84 seasonality of the annual maximum flows (Vogel and Sankarasubramanian, 2000; Smith, 1992).
85 Anthropogenic signals/drivers such as warming temperature, urbanization, and regulation (i.e.,
86 reservoir operation) have also been attributed to the shifting seasonality in floods (Regonda et al.,
87 2005; Villarni, 2016 and references therein). Berghuijs et al. (2016) explored the influence of
88 precipitation/snow characteristics, considering it as the drivers of flood generating mechanisms,
89 on the seasonality of the annual maximum flow (AMF). Their study suggested that a
90 combination of predictors - extreme rainfall seasonality, snow dynamics, and soil moisture -
91 influence the timing of the mean annual flood across the CONUS. Changes in the seasonality,
92 particularly due to earlier melt, have been observed in the seasonal streamflow at lower
93 elevations in western US (McCabe and Clark 2005, Regonda et al., 2005). Gamble (1997)
94 considered 84 drainage basins in the southeastern United States and reported that the drainage
95 basin area influences the annual peak-flood seasonality only for one out of the five regions that
96 the study investigated. His study interpreted a strong association between drainage area and
97 spring annual peak flood at Georgia coastal plain basins as a result of high soil moisture and
98 frequent extratropical cyclone passage. For New England, Magilligan and Graber (1995)
99 investigated the influence of climate control and geomorphic variables on floods timing and
100 found that the basin size, altitude, and distance from coasts affect the strength of flood
101 seasonality across 36 gauges in New England. However, the role of the basin characteristics in
102 influencing the changes in the seasonality of AMF is not fully understood yet, as they have been
103 found to impact the AMF process (e.g., Smith, 1992; McCabe and Clark, 2005). Recently, Ye et

104 al. (2017) analyzed the seasonality of AMF in 259 natural catchments in the USA and found that
105 basins with synchronous (negatively or positively) moisture (precipitation) and energy
106 (temperature) controls (i.e., moisture and energy in phase) are dominated by climate controls,
107 whereas basins with asynchronous moisture and energy controls (i.e., moisture and energy out of
108 phase) are dominated by antecedent soil moisture storage. Petersen et al., (2012) also found that
109 seasonality of streamflow is influenced by the covariability between moisture and energy with
110 basins. Villarini (2015) addressed the impact of urbanization and regulation on the seasonality of
111 floods and found that both have an effect on the strength of the flood seasonality with wider
112 seasonal distribution under regulation.

113 Climate variables across the CONUS have experienced a significant change in their
114 frequency and magnitude over the past century. Frei et al. (2013) found evidence of increased
115 occurrence and frequency in extreme precipitation events across the northern United States,
116 potentially leading to extreme streamflow events. The US Global Change Research Program's
117 Climate Science Special Report mentioned an increase of 1.8°F (1°C) in the annual average
118 temperature over the CONUS during 1901-2016 (NCA4: Wuebbles et al., 2017). Furthermore,
119 the correlation between precipitation and temperature has weakened in the last fifty years (Das
120 Bhowmik et al., 2017). To the best of our knowledge, limited/no study has investigated in
121 understanding how changes in climate variables (precipitation/temperature) and basin
122 characteristics influence the change in the seasonality of floods based on a large number of
123 natural watersheds over the CONUS. Thus, the objectives of the current study are:

- 124 1. To provide a comprehensive understanding of the change in AMF seasonality over the
125 CONUS using 975 natural HCDN watersheds that have minimal anthropogenic influence

- 126 2. To understand how changes in climate and basin characteristics on the change of AMF
127 seasonality at a regional scale.
- 128 3. To synthesize the findings from objectives 1 and 2 for developing a regional perspective
129 on changes in flood seasonality across the CONUS.

130 To understand the changes in AMF seasonality over the HCDN stations, the current study
131 considers two attributes of the seasonality measures: the seasonality index (SI) and the mean date
132 of occurrence (DO). These attributes are based on the circular statistics originally proposed by
133 Markham (1970). Several studies have considered the circular statistics for quantifying the flood
134 seasonality, which gives a basis to quantify the flood seasonality over the CONUS (Burn, 1997;
135 Villarni, 2016; Ye et al., 2017; Blöschl et al., 2017; Berghujis et al., 2019). To address the
136 second objective, the current study performs a regression analysis to attribute the changes in
137 seasonality to the changes in climate variables and basin characteristics - basin elevation and
138 drainage area. Contrary to the previous studies on changes in flood seasonality (Villarini, 2015;
139 Li et al., 2016), this study considers 975 natural watersheds from the USGS Hydroclimate Data
140 Network (HCDN), which are minimally influenced by anthropogenic disturbances. Previous
141 studies have considered these HCDN watersheds for associating streamflow with climate
142 variability and change (Sankarasubramanian and Vogel, 2002; Oh and Sankarasubramanian,
143 2012; Seo et al., 2016). We synthesize our findings in 8 larger regions by grouping the changes
144 in seasonality from the USGS-defined 18 water resources regions over the CONUS.

145 This article is organized as follows: Section 2 provides a brief overview of the data and
146 methods considered by the current study. Following that, we present the results related to the
147 change in AMF seasonality across the HCDN basins and statistically identify the significant
148 drivers of the change in AMF seasonality. Finally, we summarize the findings with a discussion.

149 **2. Data and Methodology**

150 **2.1. Streamflow Data**

151 The annual maximum peak flow data from 975 stations were obtained from the USGS-
152 HCDN database, which represents the streamflow records for basins that are minimally
153 influenced by anthropogenic factors such as reservoir storage and groundwater pumping (Slack
154 et al., 1993; Vogel and Sankarasubramanian, 2005). For additional details regarding the HCDN
155 basins, we encourage readers to read Sankarasubramanian and Vogel (2002).

156 **2.2. Basin Characteristics Data**

157 Two basin characteristics (drainage area and elevation) for the 975 stations were
158 extracted from a watershed characteristics database developed by Kroll et al. (2004). The
159 watershed scale, considered as drainage area, is a significant factor in controlling the variability
160 in floods (Smith, 1992; Vogel and Sankarasubramanian, 2000). The elevation is primarily
161 considered since it significantly induces the form of precipitation, thereby causing the lag in their
162 response during the melt season (Regonda et al., 2002). The daily precipitation and temperature
163 for the HCDN basins were obtained by spatially averaging the gridded observed daily
164 precipitation and temperature from the archive of the Bureau of Reclamation (originally
165 developed by Maurer et al., 2002; https://gdodcp.ucllnl.org/downscaled_cmip_projections/dcpInterface.html). The daily observations were
166 processed to obtain the mean monthly maximum daily precipitation and the mean monthly daily
167 temperature series over the HCDN basins (see subsection 3.2 in detail).

169 **2.3. Estimation of Seasonality Measures**

170 Flooding of a catchment can be quantified by investigating the timing and regularity (i.e.,
171 frequency) of the AMF using the seasonality measure (Burn, 1997), which provides two

172 attributes – the seasonality index (SI) of the AMF and the mean date of occurrence of the AMF
 173 (DO), based on the circular statistic suggested by Markham (1970). To estimate the SI and DO,
 174 the date of occurrence of the AMF is first converted into the Julian date, where January 1st
 175 (December 31) is considered as day 1 (day 365/366). The Julian date of occurrence of i^{th} AMF is
 176 then converted into the angular value θ_i (in radians) using equation (1).

$$177 \quad \theta_i = (\text{Julian date})_i \left(\frac{2\pi}{\bar{m}} \right) \quad (1)$$

178 where \bar{m} is the number of days per year (365/ 366 days), and n is AMF events in a catchment
 179 ($\theta_i, i = 1, \dots, n$). Second, the seasonality index (SI), which is a dimensionless measure of the
 180 spread of the AMF, and the mean date of occurrence (DO), which is the mode of occurrence in a
 181 calendar year, are estimated using equations 2 and 3.

$$182 \quad \text{SI} = \sqrt{\bar{x}^2 + \bar{y}^2} \quad (2)$$

$$183 \quad \text{DO} = \begin{cases} \arctan\left(\frac{\bar{y}}{\bar{x}}\right) \times \frac{\bar{m}}{2\pi} & \bar{x} > 0, \bar{y} \geq 0 \\ \left[\arctan\left(\frac{\bar{y}}{\bar{x}}\right) + \pi \right] \times \frac{\bar{m}}{2\pi} & \bar{x} \leq 0 \\ \left[\arctan\left(\frac{\bar{y}}{\bar{x}}\right) + 2\pi \right] \times \frac{\bar{m}}{2\pi} & \bar{x} > 0, \bar{y} < 0 \end{cases} \quad (3)$$

$$184 \quad \text{where } \bar{x} = \frac{1}{n} \sum_{i=1}^n \cos(\theta_i); \bar{y} = \frac{1}{n} \sum_{i=1}^n \sin(\theta_i) \quad (4)$$

185 The SI ranges from 0 to 1, where 1 indicates that the AMF occurs on the same Julian date every
 186 year while zero indicates that the occurrence of AMF is equally likely throughout the year
 187 (Berghuis et al., 2019). Previous studies (Burn, 1997; Petersen et al., 2012; Almanaseer and
 188 Sankarasubramanian, 2011) have shown that basins with an SI below 0.15 have no pronounced
 189 seasonality. Thus, a higher value of SI denotes a greater regularity in the AMF time of
 190 occurrence.

191 **2.4 Changes in the SI and DO**

192 The current study estimates the changes in SI and DO for two periods; hence, the
 193 identification of the change-point year is crucial. Several studies have subdivided the observed
 194 AMF by selecting a change-point year for quantifying the temporal changes in flood patterns
 195 between two periods. Coopersmith et al. (2014) and Dhakal et al. (2015) considered 1980 as the
 196 change-point year while analyzing the AMF and the annual maximum precipitation, respectively.
 197 Ye et al. (2017) adopted a varying change-point year (1970, 1975, and 1980) to analyze the
 198 changes in flood seasonality and found a limited difference in the same with the change-point
 199 year between 1970-1980. The current study performed a change point analysis (for details, see
 200 Lavielle, 2005) to identify the representative change-point year of AMF for 975 stations (Figure
 201 SI-1 in Supplementary Information). Based on the analysis, the change-point year was
 202 considered as 1970 for this study, with the average number of years before and after the change-
 203 point year being 35.54 and 40.14 years, respectively. Subsequently, the SI and DO values for the
 204 two periods, prior to 1970 and post 1970, at each HCDN station were estimated to evaluate the
 205 changes in seasonality and to quantify the shift in DO.

$$206 \quad \Delta SI = SI^{post1970} - SI^{prior1970} \quad (5)$$

$$207 \quad \Delta DO = \begin{cases} (DO^{post1970} - DO^{prior1970}) & \text{if } |DO^{post1970} - DO^{prior1970}| \leq \pi \\ (DO^{post1970} - DO^{prior1970}) + 2\pi & \text{if } (DO^{post1970} - DO^{prior1970}) < -\pi \\ (DO^{post1970} - DO^{prior1970}) - 2\pi & \text{if } (DO^{post1970} - DO^{prior1970}) > \pi \end{cases} \quad (6)$$

208 A positive difference in SI between post-1970 and pre-1970 indicates that the AMFs have
 209 become concentrated, while a negative difference in SI denote AMFs have
 210 dispersed/diffused/spread post-1970. Similarly, an increase and decrease in the DO indicate later
 211 flood arrival (LFA) and early flood arrival (EFA), respectively. To illustrate the association
 212 between AMF variability (concentrated or diffused) between two periods and the corresponding
 213 change in SI, we plotted the AMFs against calendar days for two stations with substantial

214 increase (Figure 1a) and decrease in SI (Figure 1b). For the first station (located at Big Pipe
215 Creek at Bruceville, Maryland (MD)) in region 1, the SI has increased by 0.439 by post-1979;
216 whereas, for the second station (located at Cowanesque River near Lawrenceville, Pennsylvania
217 (PA)) in region 1, it has decreased by 0.52. Figures 1a and 1b confirm that AMF occurrence is
218 dispersed (concentrated) as post-1970 value of SI becomes smaller (larger) than pre-1970 value
219 of SI. We note that a larger value of SI indicates an increase in the time from the first occurrence
220 to the last occurrence of AMF. Hence, change in SI indicates a range of AMF occurrence in a
221 calendar year. In the current study, if the absolute change in the SI from pre-1970 to post-1970 is
222 more than 0.15, the basin is assumed to have experienced a significant change in its AMF
223 occurrence. Similarly, a change in the DO for more than one month (i.e., $|\Delta DO| \geq 0.5164 \approx 30$
224 days) in its absolute value was considered as significant in terms of AMF time of arrival. Further,
225 the study has divided 975 HCDN stations into eight groups based on the hydroclimate regions in
226 which these stations are located. Group 1 consists of the Water Resources Region (WRR) 1 and
227 2, Group 2: WRR3 and WRR6, Group 3: WRR4 and WRR5, Group 4: WRR7, WRR9, and
228 WRR10, Group 5: WRR8, WRR11, and WRR12, Group 6: WRR13, WRR14, WRR15 and
229 WRR16, Group 7 is WRR17 and Group 8 is WRR18. For the ease of understanding, above eight
230 groups are referred to as Mid-Atlantic and New England (Group 1); Southeast and Tennessee
231 (Group 2); Ohio and Great Lakes (Group 3); Upper Mississippi and Missouri (Group 4); Texas
232 Gulf, Arkansas, and Lower Mississippi (Group 5); Colorado and Great Basin (Group 6);
233 Northwest (Group 7); and California (Group 8).

234 **2.5 Associating the drivers with the changes in flood seasonality – Regression analysis**

235 To address the second objective of this study, we developed a regression model with the
236 changes in AMF seasonality, SI, as the predictand and a set of climate variables and basin

237 characteristics as the predictors. Selection of potential predictors for flood seasonality relied on
238 our current understanding of the predictors of flood generation. Event rainfall, antecedent soil
239 moisture, snowpack are traditionally considered as predictors of the magnitude of flood (Parajka
240 et al. 2010, Froidevaux et al. 2015, Berghuijs et al. 2016). However, there is an absence of
241 sufficient knowledge regarding the potential predictors for flood seasonality in literature since
242 limited flood records typically restrict a comprehensive analysis attributing the changes in
243 climate and land use changes to the changes in flood characteristics (Franks and Kuczera 2002,
244 Kundzewicz et al. 2014). Blöschl and Montanari (2010) found that changing climate conditions
245 potentially impacted the magnitudes of maximum annual flood in the Danub river at Vienna,
246 Austria in the late nineteenth century. Cunderlik and Ouarda (2009) reported a weak association
247 between climate variability and/or change and the timing of flood with an early occurrence of
248 snowmelt floods. However, Berghuijs et al. (2016) found that rainfall characteristics alone are
249 unable to explain the regional patterns of seasonality and interannual variability of annual
250 maximum flows, indicating a prominent role of antecedent storage and snowmelt on flood
251 seasonality. We initially explored the previous month streamflow based on the DO as a surrogate
252 for antecedent storage; however, it did not improve the relation, and hence we dropped it in
253 developing regression. Further, our interest is in explaining the change in flood seasonality as
254 opposed to mechanisms that cause flood seasonality. We also considered drainage area as it has
255 been shown to explain the variability in AMF (Smith, 1992; Vogel and Sankarasubramanian,
256 2000). Additionally, we considered elevation as another predictor in explaining the spatial
257 variability in SI as higher elevations as it impacts the form the precipitation (i.e., rain/snow)
258 (McCabe et al., 2007). Similar to Ye et al., (2017), we also considered aridity index as an index
259 of long-term water and energy balance and also correlation between monthly precipitation and

260 temperature as a variable representing moisture and energy being in-phase (i.e., positive
261 correlation) and out-of-phase (i.e., negative correlation) within the year. However, both aridity
262 index and correlation between monthly precipitation and temperature did not play a significant
263 role in developing the best-fitting regression (results not shown), hence not included in the
264 results. We provide additional comments about this in the discussion section.

265 Considering these, two climatic attributes, changes in the mean monthly maximum daily
266 precipitation (ΔP) and the mean monthly daily temperature (ΔT), between the post-1970 and pre-
267 1970 periods have been considered as the predictors along with drainage area (DA) and elevation
268 (Elev). For calculating ΔP and ΔT for each basin, first, the month in which DO falls pre-1970 for
269 a given basin was identified. Following this, the daily precipitation/temperature for that month
270 was extracted and the maximum value was noted for each year. The mean of daily maximum
271 precipitation/temperature pre-1970 and post-1970 was then estimated and the difference in the
272 mean monthly precipitation/temperature ($\Delta P/\Delta T$) was calculated for each basin. Hereafter,
273 changes in the mean monthly maximum daily precipitation (ΔP) and the mean monthly daily
274 temperature (ΔT) are referred to as changes in precipitation and changes in temperature,
275 respectively. Further, for each WRR group, two separate regression relationships have been
276 developed between the predictand (either with basins that experienced an increase in their SI or
277 basins that experienced a decrease in their SI within a region) and the predictors and the best-fit
278 model was identified based on all the possible combinations of the four predictors using the
279 Akaike Information Criteria. An attribute/predictor is considered to influence the change in the
280 SI when the slope of regression is found to be statistically significant, with a p -value lesser than
281 0.1. Further details regarding the regression analysis are discussed in the results section and in
282 Table 1.

283
284
285
286
287
288
289
290
291
292
293
294
295
296
297
298
299
300
301
302
303
304
305

3. Results

3.1 Results for change in the seasonality

Results related to the changes in the DO (ΔDO) between the pre-1970 and the post-1970 periods for 975 HCDN stations across eight WRR groups are shown in for lower elevation ($\leq 1000\text{m}$) (Figures 2a) and higher elevation ($> 1000\text{m}$) (Figure 2b). Stations exhibiting EFA ($\Delta DO \leq 30$ days) were plotted in red, LFA ($\Delta DO > 30$ days) in green, and stations with no significant changes in their DO post-1970 (i.e., within one month) were shown as gray. Similarly, changes in the SI (ΔSI) are plotted in Figures 3a and 3b for lower and higher elevations, respectively. Significant increase (decrease) in the SI is marked with a green-triangle (purple-triangle) in Figure 3, whereas a moderate but significant change is marked by either green or purple circles. An absolute value of 0.15 was considered as a significant change in the SI between two periods. Further, to understand the changes in AMF seasonality and flood arrival since 1970, the study plots the percent change in AMF occurrence between post- and pre-1970 for twelve months (Figures 4a to 4h for the eight WRR regions). Change in the AMF occurrence for a given month is estimated as the delta change in the spatially averaged SI values across the stations whose DO earlier rested on that particular month. A positive (negative) change in Figure 4 indicates that post-1970, the AMF occurrence for a given month has increased (decreased), signifying a higher (lower) number of floods post-1970. Additionally, actual values of DO and SI for pre-1970 and post-1970 are plotted in Figures 5 and 6 respectively for each region. Basins that have DO within 30 days fall within the white portion (Figure 5), which is similar to basins shown in gray circles in Figure 2, but Figure 5 provides the season of occurrence for both pre-1970 and post-1970 for each group along with LFA and EFA based on the pre-1970 season of

306 occurrence. Similar to Figure 5, Figure 6 shows the actual SI values for pre-1970 and post-1970
307 for each group with the white region indicating no changes in SI ($|\Delta SI| < 0.15$) with basins
308 falling under increase/decrease in SI. Basins are classified based on low/high elevation in Figures
309 5 and 6.

310 Overall, based on Figures 2 and 5, very few basins experience change in DO beyond one
311 month (around 15%). Basins west of the continental divide (Groups 6-8) don't show any change
312 in DO except higher elevation basins in CA, which exhibit a LFA. Basins east of the continental
313 divide show both LFA and EFA (Figures 2 and 5) in higher and lower elevations but looking at
314 the pre-1970 and post-1970 comparative plots (Figure 5) show the changes in DO is within 30-
315 60 days in Groups 3-5. In Group 1, Mid-Atlantic and New England, changes in DO occurs
316 mostly in lower elevation with both LFA and EFA (Figure 5). In Group-2, Southeast and
317 Tennessee, AMF exhibits EFA and LFA only in higher elevation basins with limited changes in
318 lower elevation in basins. Our overall observation over the CONUS, compared to the western
319 US, significant changes in DO occurs mostly in the eastern US particularly in Groups 1-2.

320 We found that around 45% (14%) of the stations in the mid-Atlantic and New England
321 exhibit a decrease (increase) in SI post-1970. AMF occurs mostly in the winter months in the
322 mid-Atlantic and New England region, with few stations along the Appalachian exhibiting late
323 flood arrival (LFA) from winter to spring post-1970 (Figure 2a and Figure 4a). Within Group 1,
324 majority of the higher elevation basins in the Appalachian range exhibit a decrease in their SI
325 with no changes in the DO, though a few basins witness early flood arrival (EFA). Lower
326 elevation basins located in the Northeast with decreasing SI experienced shift in AMF
327 occurrence to June from March during post-1970 (Figure 4a). Under Group-2, an increase in the
328 SI is observed for the large coastal in the lower elevation basins of the Southeast with the AMF

329 occurring in the winter. Whereas, higher elevation basins located over the Southern Appalachian
330 Mountains and lower elevation basins over Florida exhibit a decrease in their SI. This primarily
331 happens with the AMF occurrence increasing in the winter (January and February) and
332 decreasing in the spring and fall (April to September) for stations across the Southwest and
333 Tennessee regions where the SI registers an increase (Figure 4b). For basins with decreasing SI
334 across the Southwest and Tennessee regions, AMF occurrence decreases in the winter and
335 increases in the spring.

336 We found that basins across the Ohio and Great Lakes region (Group 3) are mostly
337 winter dominated, with almost half of the basins exhibiting a reduction in their SI post-1970. A
338 decrease in the SI over Ohio and the Great Lakes occurs due to the decrease in AMF occurrence
339 in the winter months (Jan-March) and an increase in AMF occurrences from May to December
340 (Figure 4c). An almost equal number of basins (between 10-20%) across the Upper Mississippi
341 and Missouri region (Group 4), a spring-melt dominated region, experienced mostly decrease in
342 their seasonality index. With the exception of four basins experiencing increase in SI, lower
343 elevation basins exhibiting a decrease in their SI are typically located in the eastern part of the
344 upper Mississippi river basin and over the lower Missouri river (Figure 3a). Decrease in SI
345 occurs in lower elevation primarily due to the shift in AMF occurrence from spring to summer
346 months reduced. However, higher elevation basins under Group 4 has experienced an increase in
347 the SI (Figure 3b) and this happens due to increased AMF occurrence in the spring season
348 (Figure 3d).

349 Half of the basins in the Texas Gulf, Arkansas, and Lower Mississippi (Group 5)
350 experience mostly a decrease in SI occurs (Figure 3). Decrease in SI mostly occurs due to the
351 reduction in spring flood occurrence (Figure 4e). The majority of the basins that exhibit a

352 decrease in their SI also observed early flood arrival. Increase in SI mostly occurs in higher
353 elevation basins. Basins located in Group-6 (Colorado and Great Britain), which is a spring-
354 dominated region, typically did not exhibit any change in the seasonality of AMF. Similar results
355 were found for the snowmelt dominated basins located in the Northwest (Group 7) and
356 California (Group 8) regions, typically exhibiting a no-change in the SI. However, a decrease in
357 SI is observed for a few higher elevation basins in the Northwest and CA regions, which was
358 also reported by Pryor and Schoof (2008). Such basins experiencing decrease in SI show shift in
359 the AMF occurrence from the spring season to fall season. (Figure 4g, 4h). To summarize, the
360 changes in SI is more predominant over the east of the continental divide, whereas the SI
361 decreases in the west particularly in the higher elevation.

362 **3.2 Changes in Flood Seasonality – Attributing the Drivers**

363 Referring to Figures 2-4, the selected HCDN basins over the CONUS can be subdivided
364 into three categories based on the changes in their SI and DO: 1) change in $|SI| < 0.15$ and
365 $|DO| < 30$ days: these stations were assumed to experience no seasonality change in their AMF,
366 2) increase in SI (i.e., flood peaks are concentrated in the later period) > 0.15 or
367 SI increase < 0.15 (i.e., flood peaks are diffused in the later period) and $|DO| > 30$ days, 3)
368 decrease in SI by more than 0.15 or $|DO| > 30$ days and SI decreased by less than 0.15.
369 Considering that a few stations (15%) exhibit changes in their DO and the changes in SI is the
370 primary factor to quantify the AMF seasonality, the stations from category 1 (change in $|SI| <$
371 0.15 and $|DO| < 30$ days) were excluded from regression analysis that identifies drivers of
372 changes in SI over the CONUS. The majority of the stations that exhibit changes in DO are from
373 the mid-Atlantic and New England region (30%) located near the coastal regions or from the
374 Texas Gulf, Arkansas, and Lower Mississippi region (27%). Two regression models are

375 developed for each WRR group with the predictors being either the increase in SI across the
376 stations in category 2 (i.e., increase in SI > 0.15 , or SI increase < 0.15 , and $|DO| > 30$) or
377 decrease in SI across the stations in category 3 (i.e., decrease in SI by more than 0.15, or
378 $|DO| > 30$ days and SI decreased by less than 0.15). Table-1 provides synthesis from the
379 regression analysis with a set of identified influential attributes for each WRR group.

380 The study found that the decrease in SI for the stations located in the mid-Atlantic and
381 New England region potentially resulted from an increase in temperature (Table 1). In general,
382 an increase in the temperature results in reduced runoff potential which eventually diffuses the
383 seasonality of the AMF. An increase in temperature in the winter is linked with early snowmelt
384 for higher elevation basins located in the mid-Atlantic and New England region. However, given
385 the increase in SI across the mid-Atlantic and New England region is influenced by the increase
386 in temperature at the lower elevation basins resulting in potential delay in flood arrival (LFA).
387 For basins in Group2 (Southeast and Tennessee regions), our analysis show that a decrease in
388 precipitation is associated with a decrease in SI in the winter, while an increase in temperature
389 leads to increase in SI, which occurs mostly in the lower elevation basins (Figures 3a, 6b).
390 Analysis of the drivers for the Southeast and Tennessee regions is consistent with Kunkel et al.
391 (2010) who show the increase in the winter precipitation and temperature over the region.

392 Under Group 3, higher elevation basins show an increase in precipitation resulting in a
393 decrease in SI. Lawrimore et al. (2014) noted an increase in snowstorms in the winter; hence,
394 winters have become colder across the Ohio and Great Lakes region. This has caused higher
395 snowmelt in spring, leading to an increase in flow during the spring and summer seasons. We
396 also found that a decrease in spring precipitation potentially results in the decrease in SI for
397 basins located over the upper Mississippi and Missouri region (Group 4). A decrease in spring

398 precipitation and an increase in summer precipitation has together resulted in the dispersion of
399 AMF (as shown in Figure 4d), thereby resulting in a decrease in SI. Basins with an increase in SI
400 for group 4 are potentially influenced by the increase in spring precipitation (earlier reported by
401 Kunkel et al., 2010) which leads to the flood arrival in May. An increase in spring precipitation
402 in the northern US has been reported in the Fourth National Climate Assessment report with
403 greater increase in winter and spring precipitation in the northern and eastern US as compared to
404 the South and the West (Kunkel et al., 2010, Easterling et al., 2017 in Climate Science Special
405 Report: Fourth National Climate Assessment, Volume I). For basins located in the Texas Gulf,
406 Arkansas, and Lower Mississippi region (Group 5), a decrease in precipitation results in a
407 decrease in the SI during spring months. For Northwest basins (Group 7), decrease in SI occurs
408 with higher elevation basins. For basins in California (Group 7), decrease in precipitation across
409 the higher elevation basins) is associated with a decrease in SI, even though a change in the DO
410 was not witnessed. For basins across California that historically experience spring-melt and
411 exhibit an increase in SI, early snowmelt is triggered by the increase in winter temperature and
412 precipitation (Table 1), but the number of basins that experience a significant change in SI is
413 very small (11 showing increase in SI and 8 showing decrease in SI). To summarize, the changes
414 in SI under the considered two categories were attributable to the drivers – ΔP , ΔT , area and
415 elevation – over the eastern US (Groups 1-4). Since the number of basins experiencing a
416 significant change in SI is lesser for Groups 5-8, we could not attribute the change in SI to the
417 selected drivers.

418 **4. Discussion and Concluding Remarks**

419 The current study investigated the changes in AMF seasonality and attributed those
420 changes to four predictors – changes in the climate (ΔP and ΔT), basin characteristics (elevation,

421 and drainage area) – over 975 HCDN stations across the CONUS. To summarize, changes in DO
422 is not substantial across the CONUS. With regard to changes in SI, eastern basins (Groups 1-3)
423 are experiencing substantial changes in their SI as compared to basins in the western/central US.
424 Major findings on SI, presented in Figures 2 and 3 and Table 1, for each group are as follows:

425 a) In the Mid-Atlantic and New England regions, SI mostly decreases potentially due to
426 increase in temperature at higher elevations.

427 b) Over the Southeast and Tennessee regions, the SI has both increased and decreased in
428 a significant number of basins. Increase in SI is associated with increased temperature. Decrease
429 in SI is more pronounced at lower elevations arising from decreased precipitation.

430 c) In the Ohio and Great Lakes region, the SI mostly decreases due to potential decrease
431 in winter precipitation leading to higher spring flow.

432 d) Upper Mississippi and Missouri regions experience decrease in SI in lower elevation
433 basins due to decrease in precipitation. Increase in SI occurs in higher elevations due to increase
434 in temperature.

435 e) Over the Texas Gulf, Arkansas, and Lower Mississippi region, floods arrive early for
436 most basins, but the change in SI is not significant and associated with any of the considered
437 predictors.

438 f) Most stations over Colorado and the Great Basin region shows no change in their SI
439 and DO.

440 g) Over the Northwest, SI decreases in few basins at higher elevations indicating
441 increased variability (i.e., diffused) in flood arrival during the later period.

442 h) In California, few higher elevation basins exhibit decrease in SI due to reduced
443 precipitation, whereas around 8 basins show increase in SI.

444 Our analysis on the role of the four predictors – ΔP , ΔT and natural logarithms of
445 elevation, and drainage area – is summarized for each group in Tables 1. Except in the case of
446 New England and Mid-Atlantic regions, in general, decrease in SI (diffused) is associated with
447 decrease in ΔP (Groups 2, 3, 4 and 8). Physical basis for the role of ΔP contributing to the
448 decrease in SI could be explained as follows: decrease in precipitation during the post-1970
449 period results in reduced moisture availability which could result in increased variability in AMF
450 occurrence (i.e., decreased SI) as the basin might have not been saturated enough to produce pre-
451 1970 pattern during the post-1970 period. Thus, decrease in precipitation results in decreased SI,
452 which occurs in Southeast and Tennessee regions (Group 2), Upper Mississippi and Missouri
453 regions (Group 4) and over California (Group 8) (Table 1). For eight basins from California,
454 increase in precipitation is associated with increase in SI. Otherwise, reduced precipitation is
455 consistently associated with decrease in SI (i.e., diffused). Increase in winter and spring
456 precipitation across the northern and eastern US has been documented in the previous studies
457 (Kunkel et al., 2010; Easterling et al., 2017), which could be attributed to the decrease in SI in
458 the eastern basins.

459 For basins with increased SI (concentrated), increase in ΔT during post-1970 seems to be
460 the primary driver, which occurs in Mid-Atlantic and New England (Group 1), Southeast and
461 Tennessee (Group 2), and California (Group 3) regions. This could be explained physically as
462 follows: Increase in ΔT during the post 1970 period indicates an increased energy availability,
463 which limits the role of storage by increasing the opportunity to early melt and
464 evapotranspiration, thereby resulting in reduced variability in AMF peaks across all the regions.
465 Thus, under these situations SI increases post 1970 compared to pre 1970 period for Mid-
466 Atlantic and New England (Group 1), Southeast and Tennessee (Group 2), and California (Group

467 8) regions. Only under Group 1, increase in ΔT in higher elevation basins results in a decrease in
468 SI. Among the basin characteristics, compared to drainage area, elevation plays a more critical
469 role in influencing the changes in SI. Basins under higher elevation shows a decrease in SI,
470 which is true for all the regions except for the Texas Gulf, Arkansas, and Lower Mississippi
471 basins (Group 4), where an increase in SI has been seen. Higher elevation basins under groups 2
472 and 4 also show an increase in their SI as they experience a more pronounced melting season.
473 Increased role of elevation primarily arises in altering the form of precipitation. The role of the
474 drainage area was found to be minimal in altering the SI of AMF. We also included both aridity
475 index and correlation between monthly precipitation and temperature, which indicate the long-
476 term and within-year moisture and energy balance respectively. However, they did not play a
477 significant role in developing the best-fitting regression hence not shown in the results.
478 Compared to past studies (Ye et al., 2017) which primarily focused on identifying the predictors
479 at the national scale, moisture and energy balance indicators – aridity index and in-phase/out-of-
480 phase seasonality – did not play a significant role in the regional synthesis. One potential reason
481 is that both these moisture and energy balance indicators may not vary significantly across the
482 basins with the grouped water resources regions. Further, our study also considered almost twice
483 the naturalized basins (975 catchments in our study vs 438 catchments in Ye et al., 2017), which
484 provided an opportunity to identify drivers from a regional synthesis. Our study underscores the
485 importance of regional analyses which highlights the significant role of change in precipitation
486 and temperature and elevation being the primary drivers in influencing the change in AMF
487 seasonality within the grouped regions.

488 Understanding the changes in AMF seasonality is crucial for projecting the AMF under
489 future climate change conditions. For instance, any effort in projecting future changes requires

490 identification of the predictors corresponding to the month during which the AMF occurs
491 (Delgado et al., 2014; Condon et al., 2015; Schlef et al., 2018). The current study provides a
492 regional perspective on the predictors that contribute to the changes in AMF seasonality and
493 identifies changes in precipitation and temperature as the major drivers. Given that most basins
494 do not experience changes in their DO, we considered predictors based on SI, which denotes the
495 variability in AMF occurrence during the post-1970 period. For estimating the changes in flood
496 risk, precipitation and temperature are the two major variables that are commonly considered
497 (Condon et al., 2015), even though other attributes such as climatic indices like ENSO indicators
498 (Schlef et al., 2018) and atmospheric predictors (Delgado et al., 2014) have also been considered.
499 Although such exhaustive analyses of predictors are beyond the scope of this study, one could
500 associate regional findings from this study for analyzing the impacts of the identified predictors
501 for quantifying the changes in flood risk (e.g., Pizarro and Lall, 2002; Sankarasubramanian and
502 Lall, 2003). The role of basin characteristics, particularly elevation, is also critical in quantifying
503 the flood risk since it controls the change in SI by the influencing the form of precipitation (i.e.,
504 rain/snow). Considering these, one could consider the climate and basin characteristics in
505 quantifying regional flood risk in a hierarchical modeling setup (Chen et al., 2014; Kwon et al.,
506 2008) to explain the changes in flood seasonality. These critical efforts could potentially provide
507 reliable information and frameworks to quantify flood risk under future climate conditions.

508

509 **Acknowledgements:** This research work is partially funded by the project NSF grants CBET-1442909
510 and CBET-0954405. The dataset and computer code used to complete the analysis in this paper can be
511 downloaded from Figshare:

512 [https://figshare.com/articles/figure/Changing_Seasonality_of_Annual_Maximum_Floods_over_the_Cont](https://figshare.com/articles/figure/Changing_Seasonality_of_Annual_Maximum_Floods_over_the_Continous_US/13203731)
513 [erminous_US/13203731](https://figshare.com/articles/figure/Changing_Seasonality_of_Annual_Maximum_Floods_over_the_Continous_US/13203731)

514

516 **References**

- 517 Almanaseer, N. and Sankarasubramanian, A. (2011). Role of climate variability in modulating
518 the surface water and groundwater interaction over the southeast United States. *Journal of*
519 *Hydrologic Engineering*, 17(9), 1001-1010.
- 520 Bell, V.A. and Moore, R.J., 1999. An elevation-dependent snowmelt model for upland Britain.
521 *Hydrological Processes*, 13(12-13), pp.1887-1903.
- 522 Berghuijs, W. R., Woods, R. A., Hutton, C. J., & Sivapalan, M. (2016). Dominant flood
523 generating mechanisms across the United States. *Geophysical Research Letters*, 43(9), 4382-
524 4390.
- 525 Berghuijs, W.R., Harrigan, S., Molnar, P., Slater, L.J. and Kirchner, J.W., 2019. The relative
526 importance of different flood-generating mechanisms across Europe. *Water Resources*
527 *Research*, 55(6), pp.4582-4593.
- 528 Berghuijs, W.R., Woods, R.A., Hutton, C.J. and Sivapalan, M., 2016. Dominant flood generating
529 mechanisms across the United States. *Geophysical Research Letters*, 43(9), pp.4382-4390.
- 530 Black, A. R., & Werritty, A. (1997). Seasonality of flooding: a case study of North Britain.
531 *Journal of Hydrology*, 195(1-4), 1-25.
- 532 Burn, D.H. (1997). Catchment similarity for regional flood frequency analysis using seasonality
533 measures. *Journal of hydrology*, 202(1-4), pp.212-230.
- 534 Chen, X., Hao, Z., Devineni, N. & Lall, U. (2014). Climate information based streamflow and
535 rainfall forecasts for Huai River basin using hierarchical Bayesian modeling. *Hydrology and*
536 *Earth System Sciences*, 18(4), 1539-1548.
- 537 Condon, L. E., Gangopadhyay, S. & Pruitt, T. (2015). Climate change and non-stationary flood
538 risk for the upper Truckee River basin. *Hydrology and Earth System Sciences*, 19(1), 159-
539 175.

540 Cunderlik, J. M., & Ouarda, T. B. (2009). Trends in the timing and magnitude of floods in
541 Canada. *Journal of hydrology*, 375(3-4), 471-480.

542 Delgado, J. M., Merz, B. & Apel, H. (2014). Projecting flood hazard under climate change: an
543 alternative approach to model chains. *Natural Hazards and Earth System Sciences*, 14(6),
544 1579-1589.

545 Easterling, D.R., K.E. Kunkel, J.R. Arnold, T. Knutson, A.N. LeGrande, L.R. Leung, R.S. Vose,
546 D.E. Waliser, and M.F. Wehner, 2017: Precipitation change in the United States. In: Climate
547 Science Special Report: Fourth National Climate Assessment, Volume I [Wuebbles, D.J.,
548 D.W. Fahey, K.A. Hibbard, D.J. Dokken, B.C. Stewart, and T.K. Maycock (eds.)]. U.S.
549 Global Change Research Program, Washington, DC, USA, pp. 207-230, doi:
550 10.7930/J0H993CC.

551 Fox, J., 2015. Applied regression analysis and generalized linear models. Sage Publications,
552 ISBN: 978-1-4522-0566-3.

553 Frei, A., Kunkel, K. E., & Matonse, A. (2015). The seasonal nature of extreme hydrological
554 events in the northeastern United States. *Journal of Hydrometeorology*, 16(5), 2065-2085.

555 Gamble, D. W. (1997). The relationship between drainage basin area and annual peak-flood
556 seasonality in the southeastern United States. *Southeastern Geographer*, 37(1), 61-75.

557 Wuebbles, D., Fahey, D., & Hibbard, K. (2017). US Global Change Research Program:
558 Climate Science Special Report.

559 Gamble, D. W. (1997). The relationship between drainage basin area and annual peak-flood
560 seasonality in the southeastern United States. *Southeastern Geographer*, 37(1), 61-75.

561 Garcia-Martino, A.R., Warner, G.S., Scatena, F.N. and Civco, D.L., 1996. Rainfall, runoff and
562 elevation relationships in the Luquillo Mountains of Puerto Rico. *Caribbean Journal of*
563 *Science*, 32, pp.413-424.

564 Jonkman, S. N. (2005). Global perspectives on loss of human life caused by floods. *Natural*
565 *hazards*, 34(2), pp.151-175.

566 Klotzbach, P. J., Bowen, S. G., Pielke Jr, R., & Bell, M. (2018). Continental US hurricane
567 landfall frequency and associated damage: Observations and future risks. *Bulletin of the*
568 *American Meteorological Society*, 99(7), 1359-1376.

569 Kroll, C., Luz, J., Allen, B., & Vogel, R. M. (2004). Developing a watershed characteristics
570 database to improve low streamflow prediction. *Journal of Hydrologic Engineering*, 9(2),
571 116-125.

572 Kunkel, K. E., Easterling, D. R., Kristovich, D. A., Gleason, B., Stoecker, L., & Smith, R.
573 (2010). Recent increases in US heavy precipitation associated with tropical cyclones.
574 *Geophysical Research Letters*, 37(24).

575 Kwon, H. H., Brown, C. & Lall, U. (2008). Climate informed flood frequency analysis and
576 prediction in Montana using hierarchical Bayesian modeling. *Geophysical Research Letters*,
577 35(5).

578 Lawrimore, J., Karl, T. R., Squires, M., Robinson, D. A., & Kunkel, K. E. (2014). Trends and
579 variability in severe snowstorms east of the Rocky Mountains. *Journal of Hydrometeorology*,
580 15(5), 1762-1777.

581 Li, W., Sankarasubramanian, A., Ranjithan, R. S., & Sinha, T. (2016). Role of multimodel
582 combination and data assimilation in improving streamflow prediction over multiple time
583 scales. *Stochastic Environmental Research and Risk Assessment*, 30(8), 2255-2269.

584 Magilligan, F. J., & Graber, B. E. (1996). Hydroclimatological and geomorphic controls on the
585 timing and spatial variability of floods in New England, USA. *Journal of Hydrology*, 178(1-
586 4), 159-180.

587 Markham, C.G. (1970). Seasonality of precipitation in the United States. *Annals of the*
588 *Association of American Geographers*, 60(3), pp.593-597.

589 Maurer, E.P., Wood, A.W., Adam, J.C., Lettenmaier, D.P. and Nijssen, B. (2002). A long-term
590 hydrologically based dataset of land surface fluxes and states for the conterminous United
591 States. *Journal of climate*, 15(22), 3237-3251.

592 Mazrooei, A., Sinha, T., Sankarasubramanian, A., Kumar, S., & Peters-Lidard, C. D. (2015).
593 Decomposition of sources of errors in seasonal streamflow forecasting over the US Sunbelt.
594 *Journal of Geophysical Research: Atmospheres*, 120(23), 11-809.

595 McCabe, G. J., & Clark, M. P. (2005). Trends and variability in snowmelt runoff in the western
596 United States. *Journal of Hydrometeorology*, 6(4), 476-482.

597 McCabe, G. J., M. P. Clark, & L. E. Hay (2007). Rain-on-Snow Events in the Western United
598 States. *Bull. Amer. Meteor. Soc.*, 88, 319–328, <https://doi.org/10.1175/BAMS-88-3-319>.

599 Nakamura, J., Lall, U., Kushnir, Y., Robertson, A. W. & Seager, R. (2013). Dynamical structure
600 of extreme floods in the US Midwest and the United Kingdom. *Journal of*
601 *Hydrometeorology*, 14(2), 485-504.

602 Oh, J., & Sankarasubramanian, A. (2012). Interannual hydroclimatic variability and its influence
603 on winter nutrient loadings over the Southeast United States. *Hydrology and Earth System*
604 *Sciences*, 16(7), 2285.

605 Ohl, C. A. & Tapsell, S. (2000). Flooding and human health: the dangers posed are not always
606 obvious. *BMJ: British Medical Journal*, 321(7270), p.1167.

607 Petersen, T., Devineni, N., & Sankarasubramanian, A. (2012). Seasonality of monthly runoff
608 over the continental United States: Causality and relations to mean annual and mean monthly
609 distributions of moisture and energy. *Journal of hydrology*, 468, 139-150.

610 Peterson, T. C., Heim Jr, R. R., Hirsch, R., Kaiser, D. P., Brooks, H., Diffenbaugh, N. S., ... &
611 Katz, R. W. (2013). Monitoring and understanding changes in heat waves, cold waves,
612 floods, and droughts in the United States: state of knowledge. *Bulletin of the American*
613 *Meteorological Society*, 94(6), 821-834.

614 Pizarro, G. & Lall, U. (2002). El Niño-induced flooding in the US West: What can we expect?.
615 *Eos, Transactions American Geophysical Union*, 83(32), 349-352.

616 Pryor, S. C., & Schoof, J. T. (2008). Changes in the seasonality of precipitation over the
617 contiguous USA. *Journal of Geophysical Research: Atmospheres*, 113(D21).

618 Regonda, S.K., Rajagopalan, B., Clark, M. & Pitlick, J. (2005). Seasonal cycle shifts in
619 hydroclimatology over the western United States. *Journal of Climate*, 18(2), pp.372-384.

620 Sankarasubramanian, A. & Lall, U. (2003). Flood quantiles in a changing climate: Seasonal
621 forecasts and causal relations. *Water Resources Research*, 39(5).

622 Sankarasubramanian, A. & Vogel, R. M. (2002). Annual hydroclimatology of the United States.
623 *Water Resources Research*, 38(6), 19-1.

624 Seo, S. B., Sinha, T., Mahinthakumar, G., Sankarasubramanian, A., & Kumar, M. (2016).
625 Identification of dominant source of errors in developing streamflow and groundwater
626 projections under near-term climate change. *Journal of Geophysical Research:*
627 *Atmospheres*, 121(13), 7652-7672.

628 Schlef, K. E., François, B., Robertson, A. W. & Brown, C. (2018). A General Methodology for
629 Climate-Informed Approaches to Long-Term Flood Projection—Illustrated With the Ohio
630 River Basin. *Water Resources Research*, 54(11), 9321-9341.

631 Slack, J. R., Lumb, A.M. & Landwehr, J.M. (1993). Hydro-Climatic Data Network (HCDN)—A
632 USGS streamflow data set for the U.S. for the study of climate variations, 1874–1988, *U.S.*
633 *Geol. Survey. Water Resources Investigation Report*, 93–4076.

634 Smith, J. A. (1992). Representation of basin scale in flood peak distributions. *Water Resources*
635 *Research*, 28(11), 2993-2999.

636 Steinschneider, S. and Lall, U. (2016). El Niño and the US precipitation and floods: What was
637 expected for the January–March 2016 winter hydroclimate that is now unfolding?. *Water*
638 *Resources Research*, 52(2), 1498-1501.

639 Villarini, G. (2016). On the seasonality of flooding across the continental United States.
640 *Advances in Water Resources*, 87, pp.80-91.

641 Vogel, R. M., & Sankarasubramanian, A. (2000). Spatial scaling properties of annual streamflow
642 in the United States. *Hydrological sciences journal*, 45(3), 465-476.

643 Vogel, R. M., & Sankarasubramanian, A. (2005). Monthly climate data for selected USGS
644 HCDN sites, 1951–1990. *Oak Ridge National Laboratory Distributed Active Archive Center*,
645 *Oak Ridge, Tennessee, USA*.

646 Wang, W., Chen, X., Shi, P. & Van Gelder, P. H. A. J. M. (2008). Detecting changes in extreme
647 precipitation and extreme streamflow in the Dongjiang River Basin in southern China.
648 *Hydrology and Earth System Sciences Discussions*, 12(1), 207-221.

649 Wasko, C., Sharma, A., & Lettenmaier, D. P. (2019). Increases in temperature do not translate to
650 increased flooding. *Nature Communications*, 10(1), 1-3.

651 World Health Organization (2002). Floods: climate change and adaptation strategies for human
652 health. *World Health Organization of the United Nations*, London.

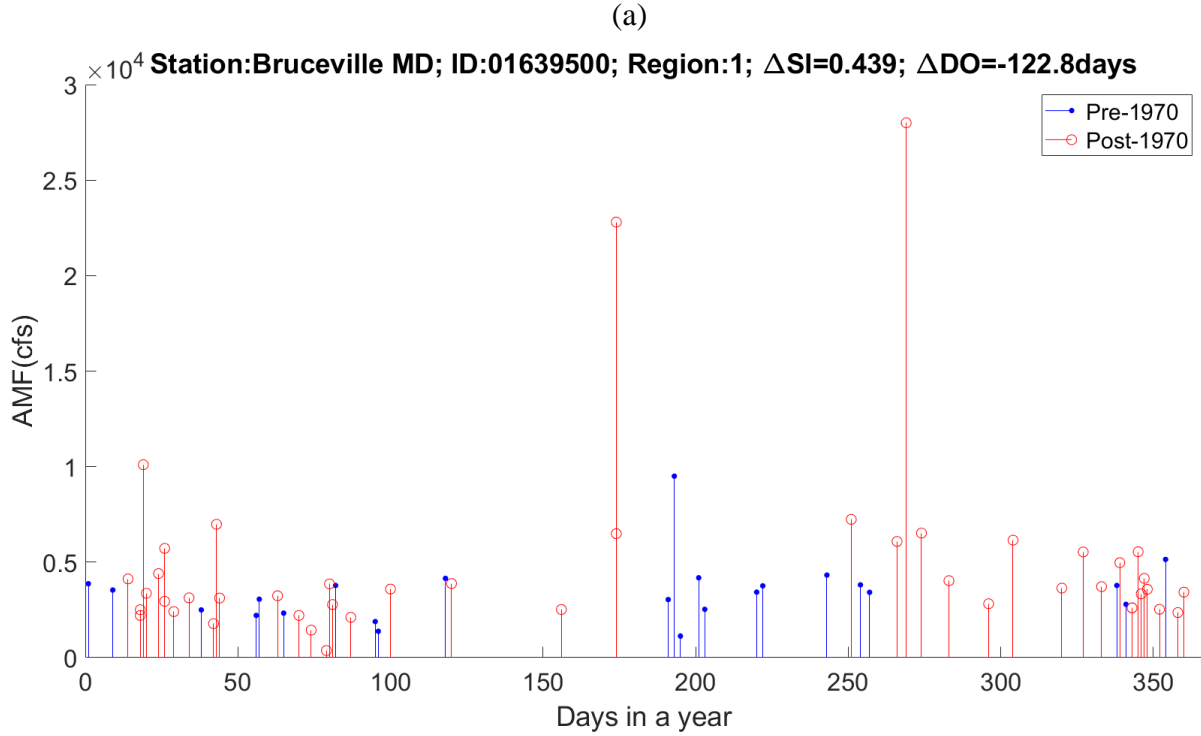
653 Wuebbles, D. J., Fahey, D. W., & Hibbard, K. A. (2017). Climate science special report: fourth
654 national climate assessment, volume I.

655 Zhu, X., Troy, T. J., & Devineni, N. (2019). Stochastically modeling the projected impacts of
656 climate change on rainfed and irrigated US crop yields. *Environmental Research Letters*,
657 *14*(7), 074021.

658 Ye, S., Li, H.Y., Leung, L.R., Guo, J., Ran, Q., Demissie, Y. & Sivapalan, M. (2017).
659 Understanding flood seasonality and its temporal shifts within the contiguous United States.
660 *Journal of Hydrometeorology*, *18*(7), pp.1997-2009.

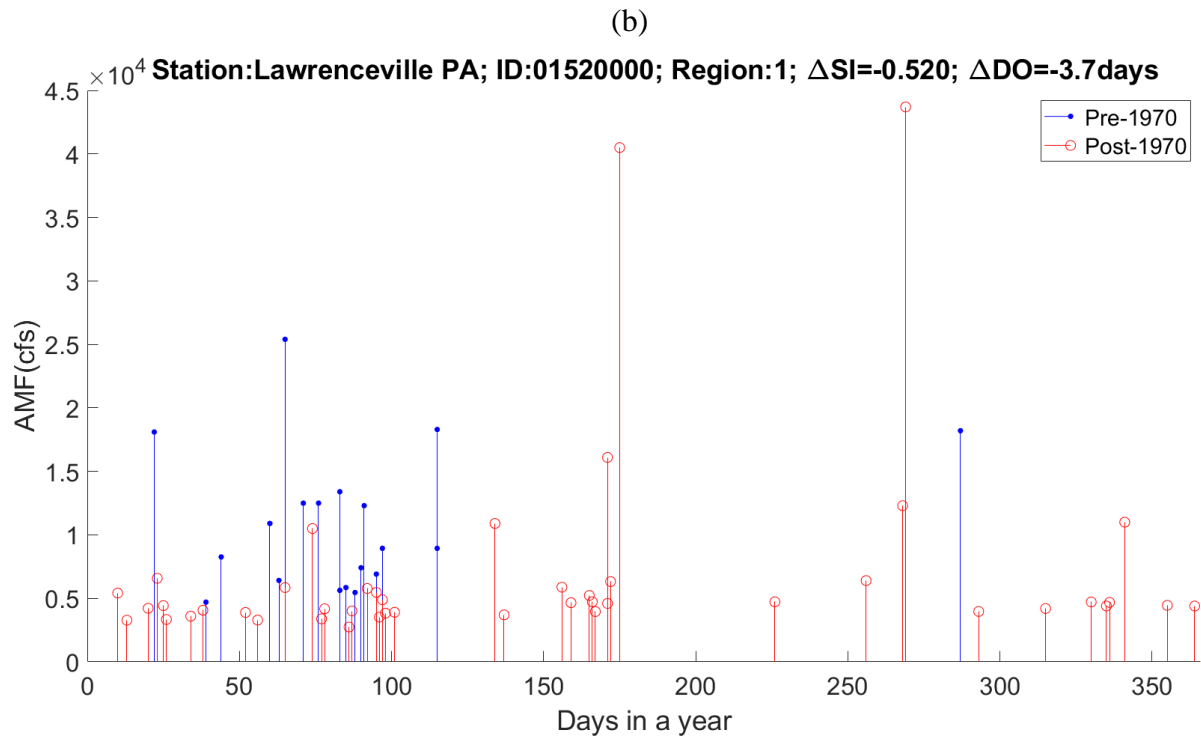
661 Yin, J., Gentine, P., Zhou, S., Sullivan, S. C., Wang, R., Zhang, Y., & Guo, S. (2018). Large
662 increase in global storm runoff extremes driven by climate and anthropogenic
663 changes. *Nature communications*, *9*(1), 1-10.

664



665

666

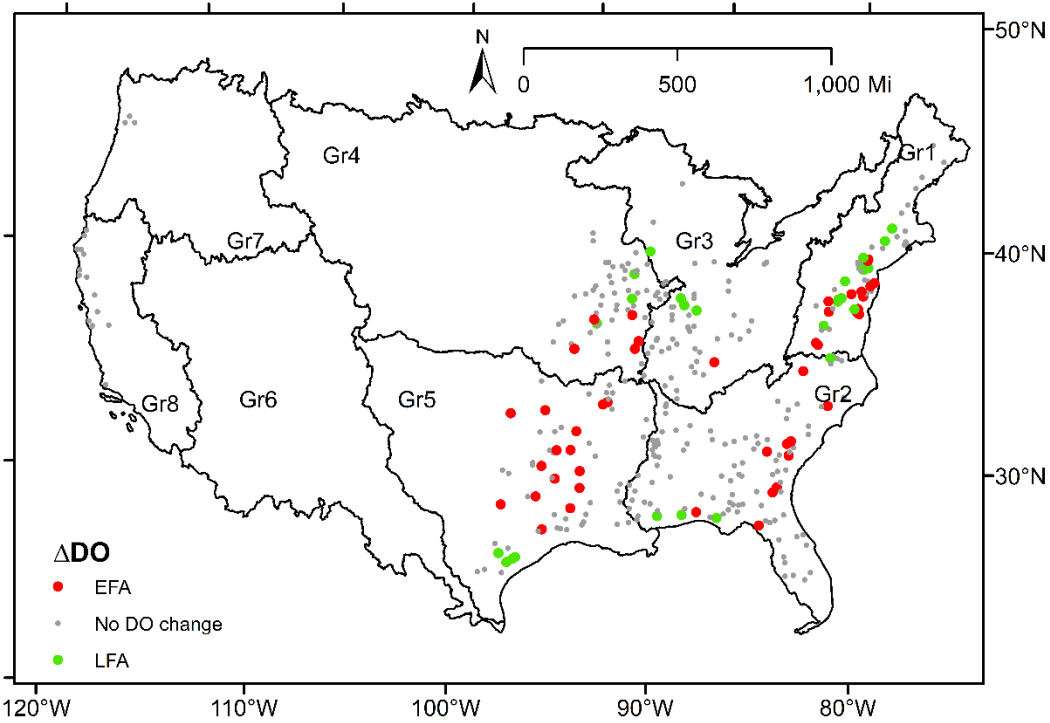


667

Figure 1. Scatter plot of AMF values (in cfs) against calendar days for two stations with (1a) increase in SI (concentrated) and (1b) decrease in SI (diffused) before and after 1970.

668

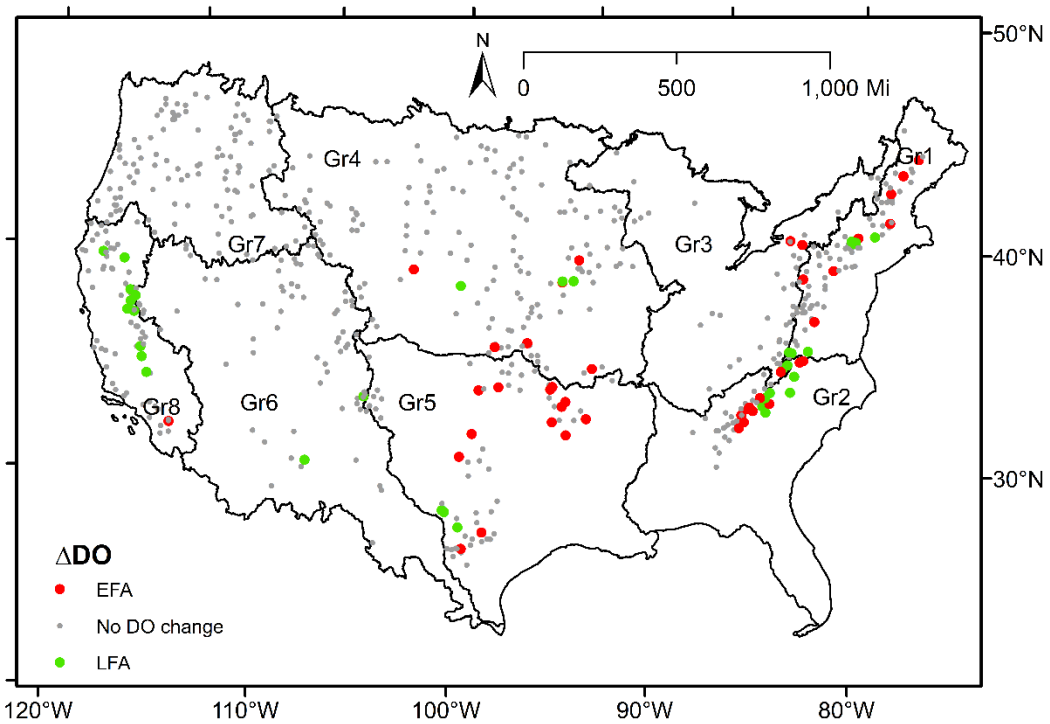
a) Lower elevation ($\leq 1000m$)



669

670

b) Higher elevation ($>1000m$)



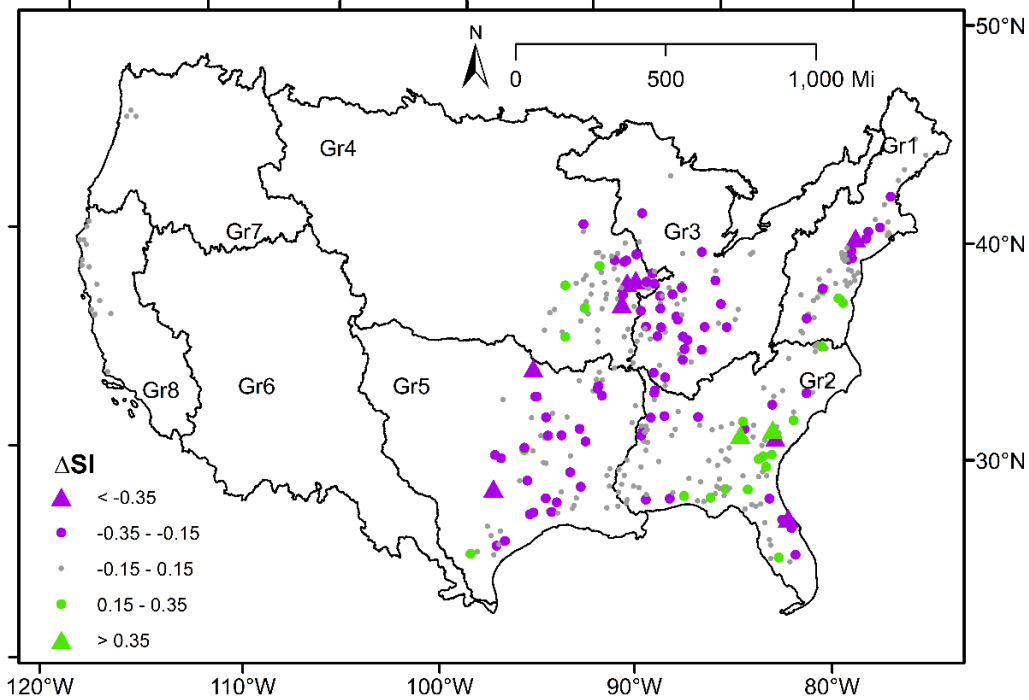
671

672

673 **Figure 2.** Changes in the dominant season of occurrence (ΔDO) of annual maximum floods between pre-
674 and post-1970 over HCDN stations under eight groups. HCDN stations are segregated based on lower and
675 higher elevations (Figures 2a and 2b respectively) Red, green and gray circles indicate stations with the
676 early arrival of floods (EFA), late arrival of floods (LFA), and no change in DO, respectively.

677

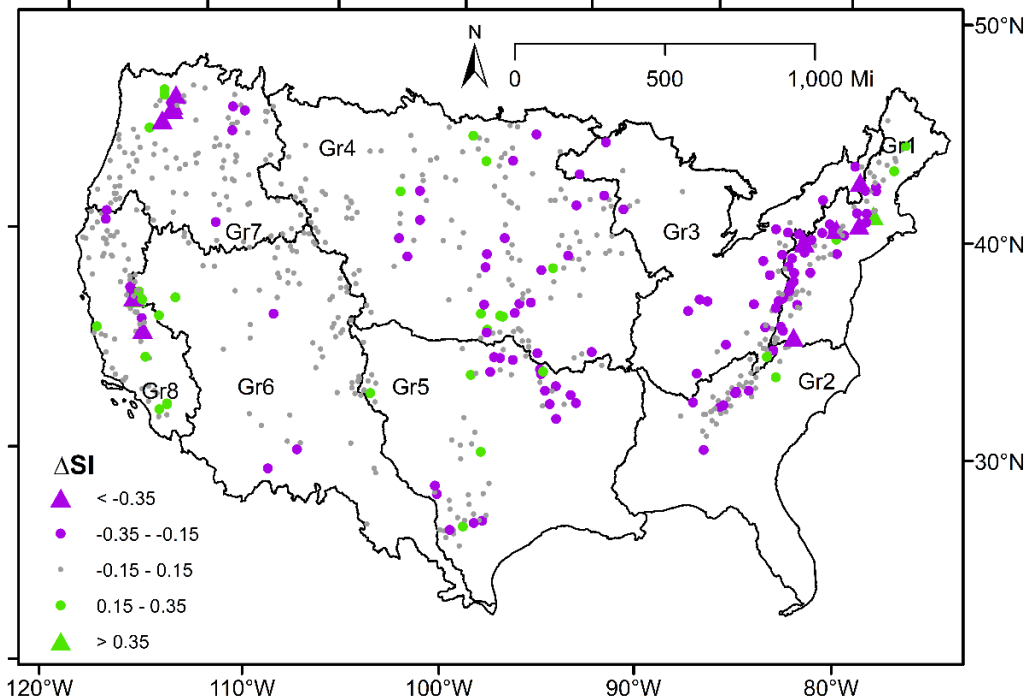
a) Lower elevation ($\leq 1000m$)



678

679

b) Higher elevation ($>1000m$)



680

681

682

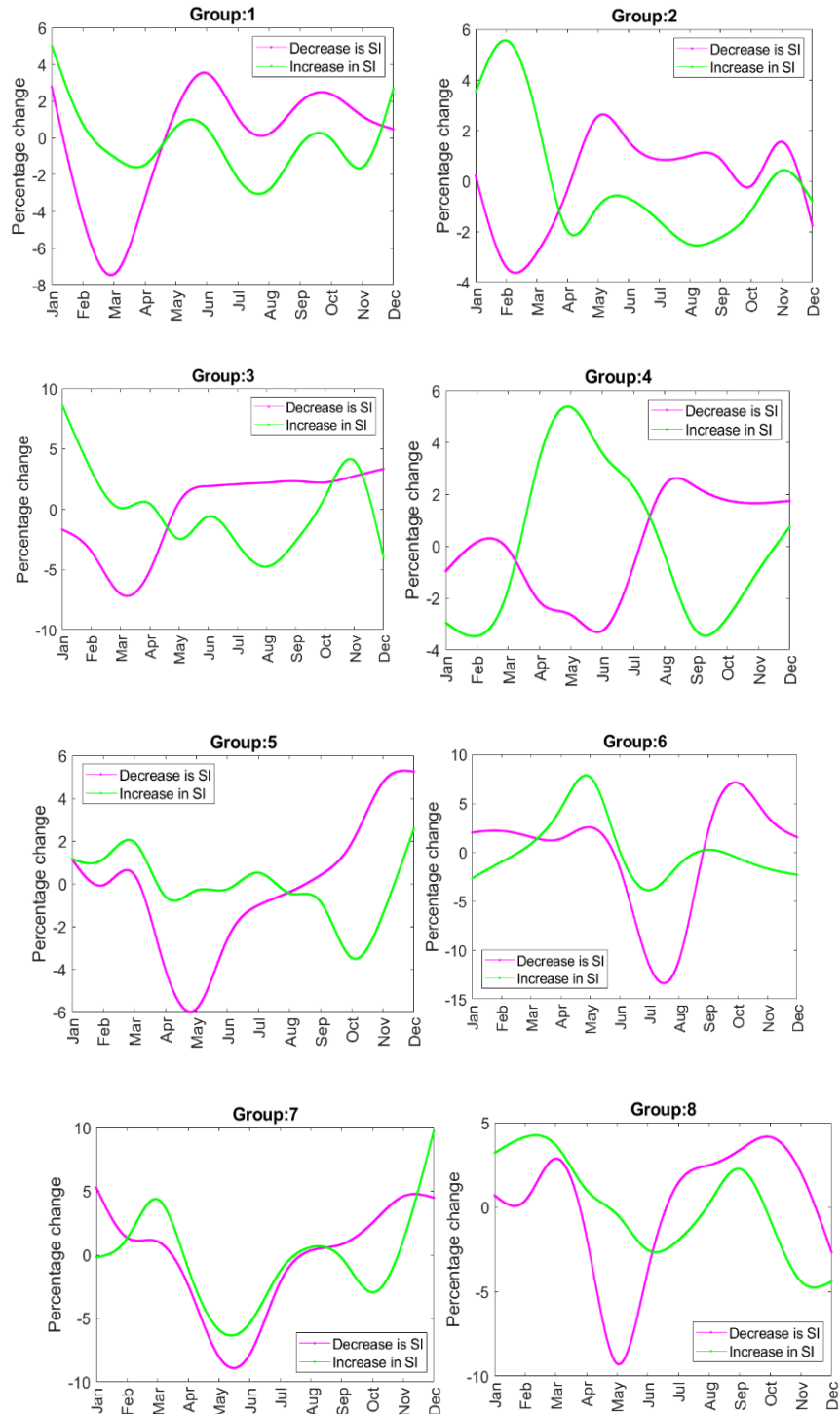
683

684

685

686

Figure 3. Changes in seasonality index (ΔSI) of annual maximum floods between pre-1970 (SI_1) and post-1970 (SI_2) over HCDN stations under eight groups. HCDN stations are segregated based on lower and higher elevations (Figures 3a and 3b respectively). Green-triangle and green-circle indicate stations where floods are more concentrated (increase in SI); while purple-triangle and purple-circle indicate stations where floods arrive more diffused (decrease in SI). Stations with no changes in the seasonality of floods over post-1970 (no change in SI) are identified in grey-dots.



687
 688 **Figure 4.** Percent change in AMF occurrence between post- and pre-1970 for eight regions and
 689 twelve months. Positive change means an increase in occurrence for the month after 1970.
 690 Change in AMF occurrence for a given month is estimated as the delta change in spatially
 691 averaged SI values across stations whose DO earlier rested on that particular month. A positive
 692 (negative) change indicates that post-1970, the AMF occurrence for a given month has increased
 693 (decreased)

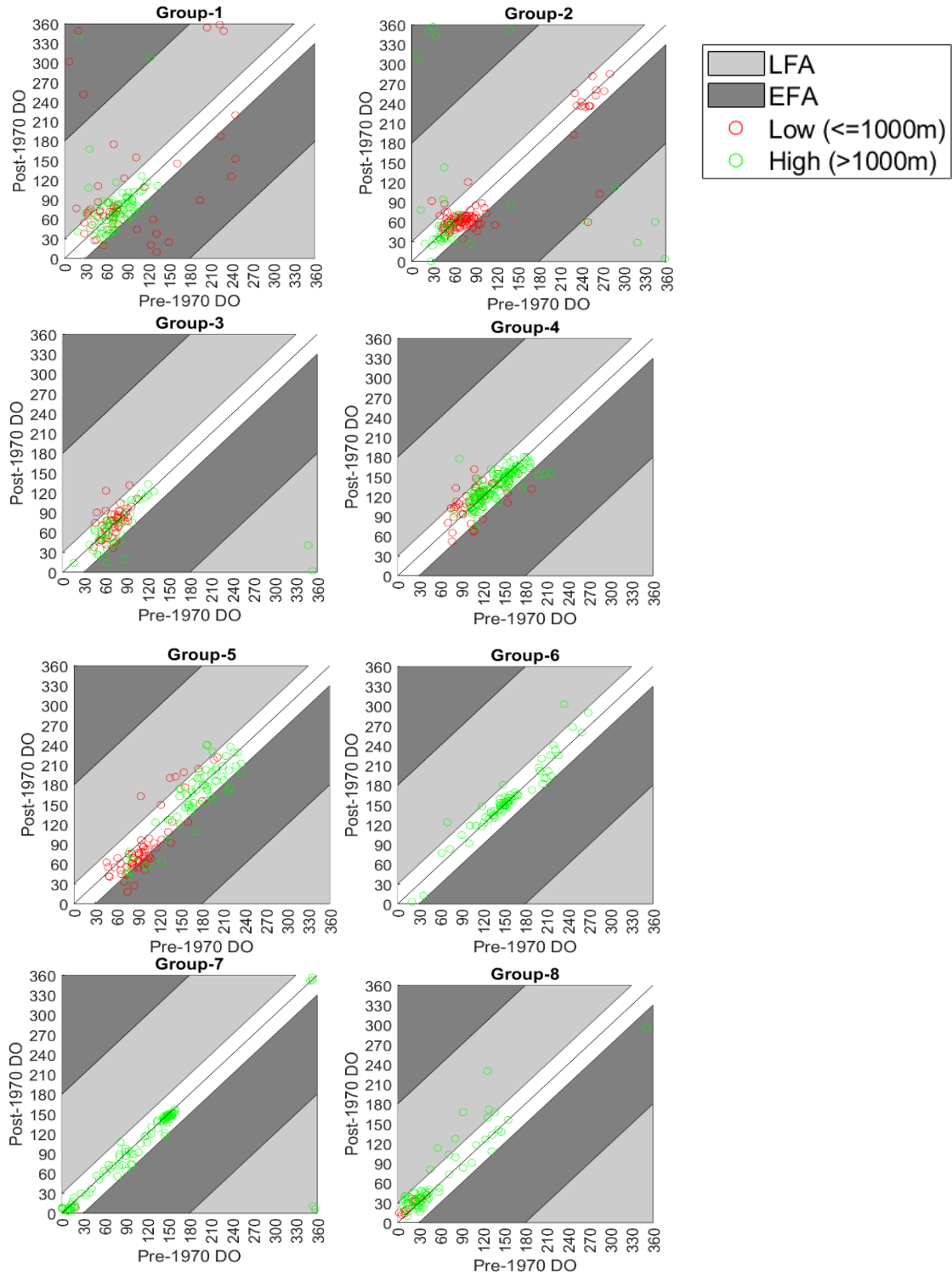
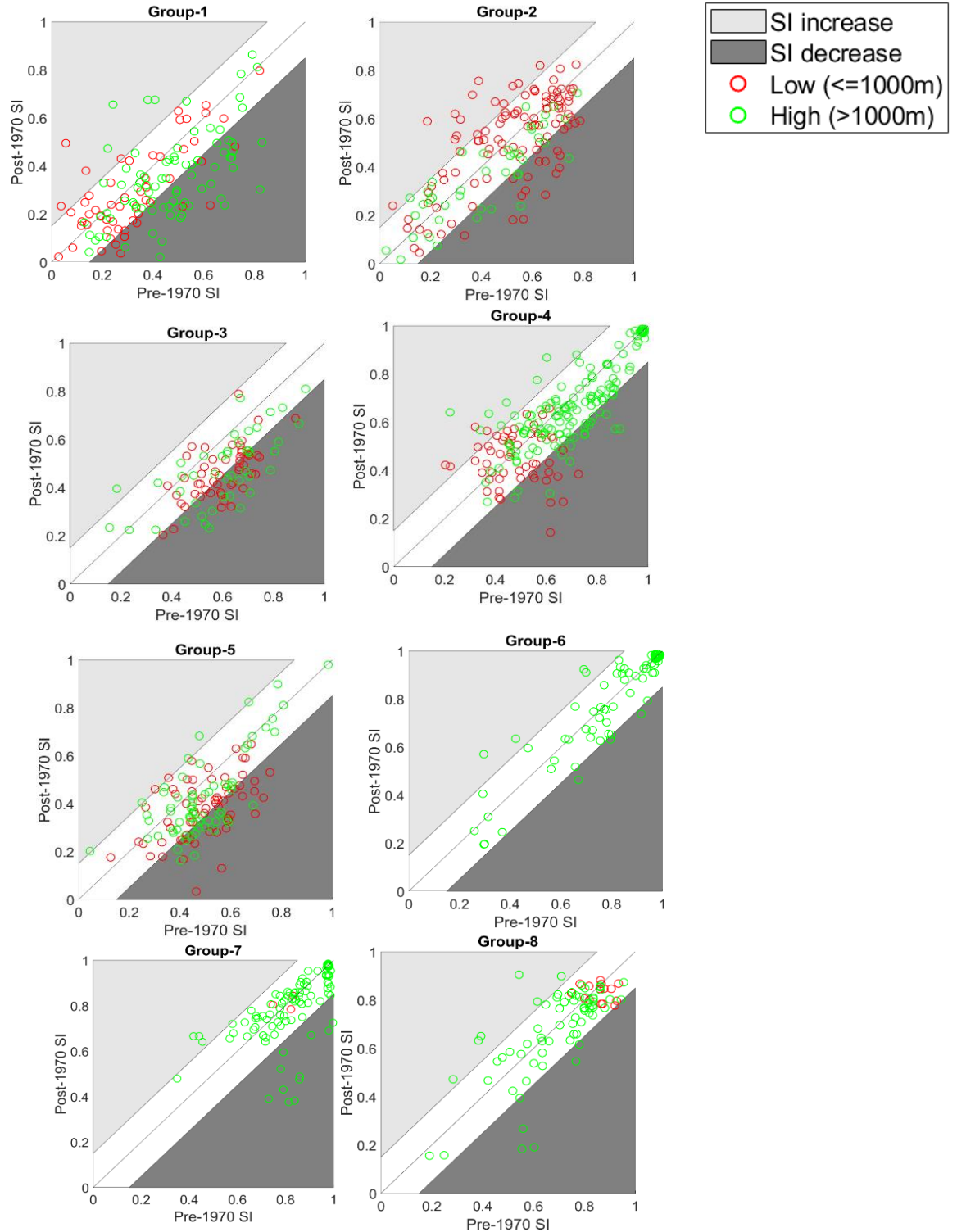


Figure 5. Values of DO of each basin pre- and post-1970. Basins falling in light gray shaded area exhibit later flood arrival (LFA) while basins in dark grey shaded area have early flood arrival (EFA) post-1970, whereas basins in the white area does not have significant changes in dO (less than 30 days). Blue circle corresponds to basins with low elevation (less than or equal to 1000m) and green circle represents basins with high elevation (greater than 1000m).



694 **Figure 6.** Values of SI of each basin pre- and post-1970. Blue circle corresponds to basins with
 695 low elevation (less than or equal to 1000m) and green circle represents basins with high
 696 elevation (greater than 1000m). Basins in light gray area exhibit increase in SI, basins falling in
 697 dark gray have decrease in SI, while basins located in the white area does not exhibit significant
 698 change in SI (less than 0.15 in absolute value).

699 **Table-1.** Hydroclimatic and watershed related attributes influencing changes in the seasonality
700 index (SI) and/or mean date of occurrence (DO) of the AMF post-1970 for each group. The
701 number of basins (#) considered in the regression, along with the change in |SI| above 0.15 and
702 the change in DO, are provided. Significant regression coefficients and their p-values (in
703 parenthesis) are provided from the best-fitting linear regression.

Group	Total stations	The slope of selected attributes and p-value		Influencing factors
		Decrease in SI (diffusion)	Increase in SI (concentration)	
1	136	#:61 ΔT : -0.059 (0.04) Elev: -0.091 (0.05)	#:19 ΔT : 0.263 (0.01)	Mostly winter dominated; both early and late flood arrival occurs <ul style="list-style-type: none"> A decrease in SI occurs with increased ΔT and at higher elevation basins An increase in the SI occurs with increased ΔT
2	151	#:38 ΔP : 0.005 (0.1) Elev: 0.049 (0.08)	#:25 ΔT : 0.057 (0.1) Elev: -0.090 (0.1)	AMF occur throughout the year; floods arrive early at lower elevations <ul style="list-style-type: none"> A decrease in SI occurs with reduced ΔP at lower elevations An increase in SI occurs with increased ΔT
3	96	#:48 Elev: -0.099 (0.05)	#:2 NA	Mostly winter dominated <ul style="list-style-type: none"> Decrease in SI is associated with increase in elevation.
4	203	#:34 ΔP : 0.010 (0.02) Elev: 0.097 (0.1)	#:21 Elev: 0.240 (0.01)	Mostly spring dominated, few stations exhibit early flood arrival <ul style="list-style-type: none"> Decrease in SI occurs with reduced ΔP and in lower elevations Increase in SI occurs at higher elevations
5	130	#:56 NA	#:11 NA	Floods arrive early; no significant drivers
6	73	#:4 NA	#:6 NA	Mostly spring dominated and no significant drivers identified.
7	103	#: 11 Elev: -1.749 (0.03)	#:3 NA	Decrease in SI for spring-melt basins; <ul style="list-style-type: none"> Decrease in SI occurs in higher elevations
8	83	#:11 ΔP : 0.018 (0.08) Elev: -0.794 (0.02)	#:8 ΔP : 0.010 (0.1) ΔT : 0.136 (0.1)	Mostly winter dominated and floods arrive late in the higher elevations <ul style="list-style-type: none"> Decrease in SI occurs with reduced ΔP in higher elevations Increase in SI occurs with an increase in ΔP and ΔT

704

705

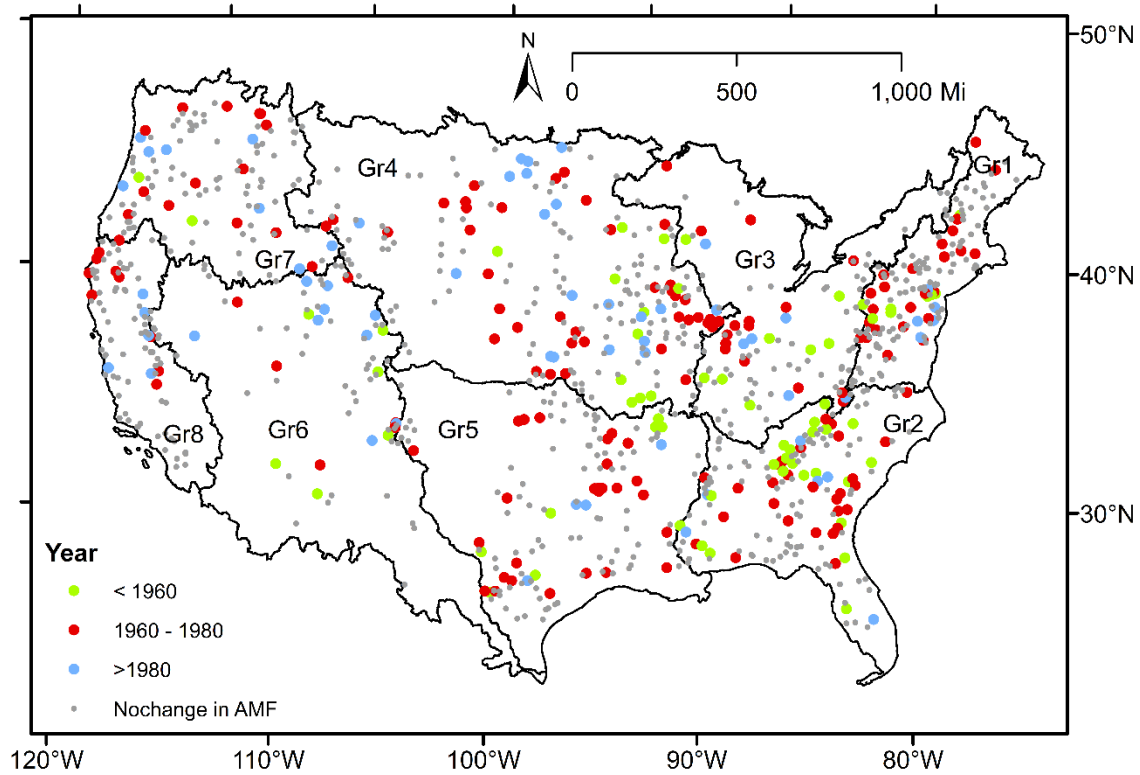
706

707

708

709

Supplemental Information



710

711 **Figure-SI-1.** Spatial variation of change-year of Annual Maximum Flow (AMF) for each on the 975
 712 stations. Stations exhibiting no change in AMF were shown in gray.

713 Details on Figure SI-1: The median of change-year for all of the 975 stations was found to be 1967,
 714 whereas for each of the group where significant changes in AMF were noted were as follows: 1965
 715 (Group-1), 1959 (Group-2), 1970 (Group-3), 1984 (Group-4), 1963 (Group-5), 1977 (Group-6), 1975
 716 (Group-7) and 1976 (Group-8).